La mer 56 : 113–123, 2018
Société franco-japonaise d'océanographie, Tokyo

# A note on the abyssal circulation in the Japan Sea: suggestion from rotating-tank experiments

Tomoharu SENJYU[1] and Jiro YOSHIDA[2]

**Abstract:** In this study, we revisited the rotating-tank experiments reported by FALLER (1960) and SENJYU (1988) and qualitatively discussed the abyssal circulation in the Japan Sea by focusing on the geometric similarity of their partial barrier experiments. A point source of water near the apex of the pie-shaped rotating-tank formed the so called STOMMEL-ARONS type circulation pattern. The circulation in the partial barrier experiments basically consisted of a cyclonic circulation and a western boundary current in the southern two basins separated by a partial barrier extending from the rim. Recent observations on direct current in the abyssal Japan Sea have revealed a cyclonic circulation and strong currents near the western boundary in the southern two basins: the Yamato and Tsushima Basins. These similarities suggest the STOMMEL-ARONS type circulation in the abyssal Japan Sea, though the complex bottom topography and eddy activity are likely to modify the basic circulation pattern significantly.

***Keywords :*** *Rotating-tank experiment, deep circulation, deep western boundary current, direct current observation*

## 1. Introduction

The oceanic abyssal circulation is one of the most important parts of the global climate system, which transports cold deep water in a high-latitude region to low-latitude areas. During the course of this circulation, cold water gradually upwells and eventually returns to the high-latitude region by the surface currents. Therefore, abyssal circulation bears the lower part of the meridional overturning or thermohaline circulation (TALLEY *et al.*, 2011).

The first dynamic model of the global abyssal circulation was presented by STOMMEL (1958) and STOMMEL and ARONS (1960a, b). Their basic concept of the global abyssal circulation (hereafter, the SA-type circulation) is as follows: the volume of cold water sunken in the high-latitude regions (the northern North Atlantic and the Antarctic) is compensated by the upwelling over the world ocean. The vertical velocity ($w$, positive upward) accompanied by the upwelling induces positive (negative) relative vorticity through stretching of water column ($f\partial w / \partial z$, where $f$ is the planetary vorticity) in the north-

1) Division of Earth Environment Dynamics, Research Institute for Applied Mechanics, Kyushu University
6–1 Kasuga-Koen, Kasuga City, Fukuoka 816–8580, Japan
E-mail: senjyu@riam.kyushu-u.ac.jp
2) Tokyo University of Marine Science and Technology
4–5–7 Konan, Minato, Tokyo 108–8477, Japan
E-mail: jiroy@kaiyodai.ac.jp

ern (southern) hemisphere. Since, in the steady state, the relative vorticity must be balanced by the advection of planetary vorticity ($\beta v$, where $\beta$ and $v$ denote meridional derivation of $f$ ($df / dy$) and meridional geostrophic velocity positive northward, respectively) to conserve potential vorticity, poleward flow appears over the interior region of each oceanic basin. To satisfy the condition of continuity, a western boundary current (WBC) is introduced toward low latitude in each basin. The basic characteristics of the SA-type circulation in the oceans, such as the deep WBC, have been validated by many researchers by using chemical tracers and neutral drifters (e.g., BROECKER and PENG, 1982; SWALLOW and WORTHINGTON, 1961).

The concept of the SA-type circulation was initiated from a rotating-tank experiment with a point source of water (STOMMEL *et al.*, 1958). Because this experiment was very simple, additional experiments were performed to examine several conditions appearing in the real ocean, for example lateral boundary (FALLER, 1960; SENJYU 1988), bottom topography (WELANDER, 1969; KUO and VERONIS, 1971), and nonlinear effects (VERONIS and YANG, 1972). In this study, we revisit the partial barrier experiments by FALLER (1960) and SENJYU (1988) and discuss the deep circulation in the Japan Sea by referring to the results of the rotating-tank experiments.

The Japan Sea has its own thermohaline circulation system with the formation of deep and bottom waters (hereafter, the Japan Sea Proper Water) which were surface water sunken in the northwestern part of the sea, south of Vladivostok (Fig. 1) (GAMO and HORIBE, 1983; SUDO, 1986; SENJYU and SUDO, 1993 & 1994; SENJYU *et al.*, 2002). In addition, the Japan Sea has southern and northern surface circulations with a WBC (the East Korean Current in the south and the Liman Current in the north) bounded by a subarctic front, similar to the subtropical and subarctic gyres in the Pacific and Atlantic oceans. This indicates that the planetary $\beta$-effect is substantially important for basin-scale circulation in the sea. These conditions make us expect the SA-type circulation in the abyssal Japan Sea. Furthermore, the bottom topography of the Japan Sea (Fig. 1) is similar to the geometry of the partial barrier experiment (Fig. 2); a northern basin *N* corresponds to the Japan Basin, and two southern basins *SW* and *SE* correspond to the Yamato and Tsushima Basins, respectively. These two basins are bounded by a shallow ridge extending from the Oki Islands to the Yamato Rise (the Oki Spur), as well as its closed configuration.

In the next section, we describe the principle and method involved in the rotating-tank experiments referring to results of the test experiments of the SA-type circulation. Section 3 introduces some results of the partial barrier experiments by SENJYU (1988) weighted on the change of flow pattern when the length and angle of the partial barrier were varied. Section 4 provides a qualitative discussion about the Japan Sea deep circulation using the analogy of the partial barrier experiments. Finally, Section 5 presents concluding remarks.

## 2. Test experiments of the SA-type circulation

Prior to the partial barrier experiments, SENJYU (1988) performed a series of test experiments of the STOMMEL *et al.*'s (1958) SA-type circulation. In this section, the principle and method of the experiments are explained referring to the results of the test experiment.

A pie-shaped tank (Fig. 2, but without the partial barrier) containing water was set on a turntable and was rotated anticlockwise with respect to the vertical axis at a constant angular velocity ($\omega$). Since the spin-up time scale $t_s = (h^2$

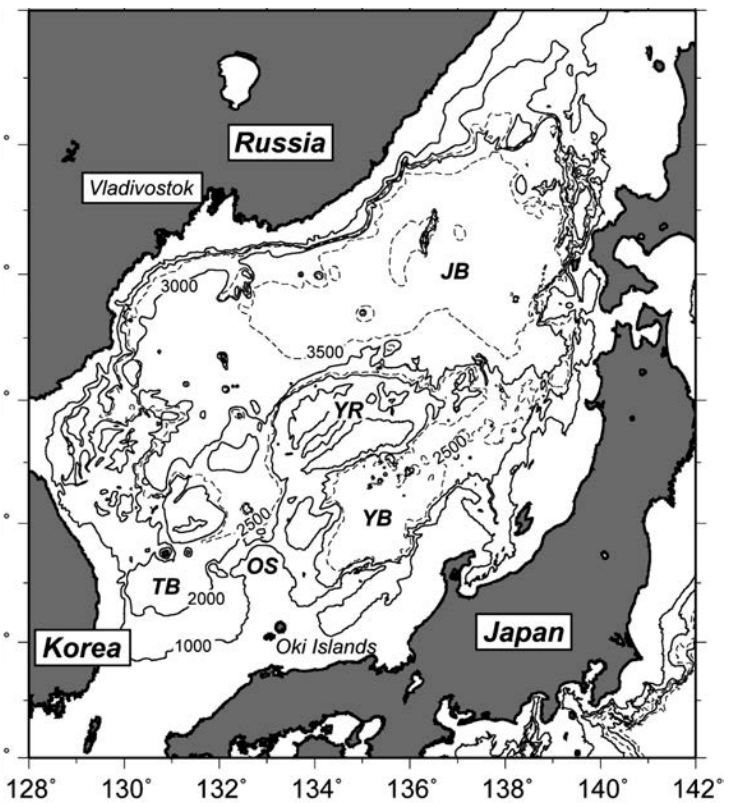


**Fig. 1** Bottom topography of the Japan Sea. *JB*, *YB*, *TB*, *YR*, and *OS* denote the Japan Basin, Yamato Basin, Tsushima Basin, Yamato Rise, and Oki Spur, respectively.

$/ \nu\omega)^{1/2}$ was estimated to be about 100 s using the water depth $h$~O (10 cm), viscosity $\nu$~O ($10^{-2}$ cm$^2$ s$^{-1}$), and $\omega$~O (1 rad s$^{-1}$), each experiment was started after an hour rotation (rigid-body rotation).

After achieving the rigid-body rotation state, a small volume of dyed water was constantly injected into the tank from a point source near the apex of the sector ($S_O$), which corresponds to a narrow source region of the deep water in the real ocean. For the dyeing of water, a small volume of brilliant-blue was used. To minimize the density difference between waters in the tank and for the injection, the waters were put in the same environment at least 12-h long before each experiment. At last, the smallness of the density difference was confirmed by vertical rigidity of the injected water during the experiments, that is, whether the injected water forms a TAYLOR's ink wall or not (*e.g.*, Long, 1954).

The outlet of the dyed water was set at 1.0–1.5 cm below the water surface under the Ekman layer; the thickness of the Ekman layer is $\delta_E = (\nu / 2\omega)^{1/2}$~O ($10^{-1}$ cm), if we adopt the above values of $\nu$ and $\omega$. In addition, the tank was covered with a clear acrylic lid to escape air stress on the water surface. The flow pattern in the tank visualized by the dyed injected water was recorded by a camera installed on the turntable.

The water level before the start of rotation

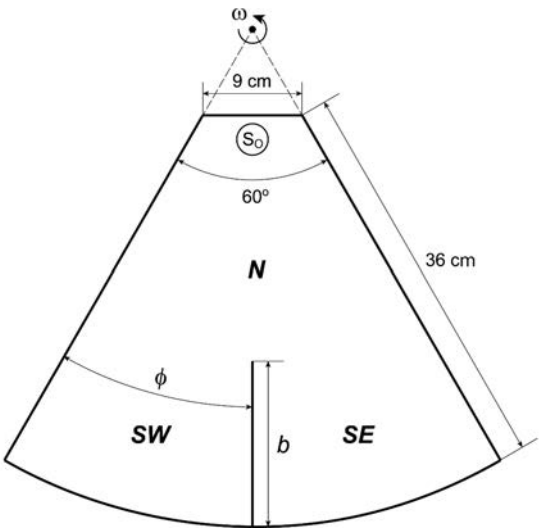


**Fig. 2** Dimension of the experiment tank. *N*, *SW*, and *SE* indicate three basins separated by a partial barrier of length $b$ and angle $\phi$ from the western boundary. $S_O$ is a point source of water. The tank is rotating anticlockwise at an angular velocity $\omega$ with respect to the vertical axis.

was set at 8.3 cm. However, the free surface of water during the experiments is a paraboloidal shape, with a minimum at the apex and a maximum at the rim, because of the balance of pressure gradient and centrifugal force. The planetary $\beta$-effect is approximately simulated by the radial variation of the water depth ($\beta \approx -2\omega\,(dh/dr)/h_0$, where $r$ denotes the radial distance from the rotating axis and $h_0$ is the water depth at $r = 0$). Hence, the apex side (rim side) of the tank corresponds to the north (south) in the real ocean, and thus, we use the words "north", "south", "east", "west", and so on to show the direction.

Since there is no sink of water in the tank, the water surface slowly rises with time in the experiments, which simulates the upwelling in the interior region of the real ocean, although STOMMEL and ARONS (1960a, b) assumed the steady state condition. This temporal change of the water level influences the planetary $\beta$-effect via the relation $\beta \approx -2\omega\,(dh/dr)/h_0\,(t)$, now $h_0$ is a function of time $t$. The injection rate of water was set at about 1.0 $cm^3\ s^{-1}$, and the duration of an experiment was about 30 min. Therefore, the volume of injected water at the end of the experiment reached 1800 $cm^3$. Since the area of the tank is 1025.2 $cm^2$, the difference of water level before and after the experiment was about 1.8 cm. This corresponds 23% of the initial water depth at the rotating axis ($h_0\,(0) = 7.8$ cm). Therefore, we should keep on mind the fact that the $\beta$-effect was reducing by about 20% during the experiment.

Figure 3 shows time sequence of a test experiment. A clockwise eddy near the point source grew gradually (Fig. 3a-b), then a narrow and fast flow along the western boundary (the WBC) appeared from the eddy (Fig. 3c-d). The dyed water flowed eastward along the southern boundary accompanying a wide but sluggish northward flow (the interior flow) after arriving at the rim (Fig. 3e-g), finally a westward intensified cyclonic gyre (the SA-type circulation) was confirmed (Fig. 3h).

STOMMEL *et al.* (1958) set the ROSSBY number $R_o = V/(2R\omega)$ ($V$ is the representative speed of the WBC and $R$ is the distance from the rotating axis to the rim of the tank, 45 cm) to be $O(10^{-3})$, the same order of magnitude as that for the Gulf Stream system. However, SENJYU (1988) adjusted $R_o$~$O(10^{-2})$ due to the limit of the experimental equipment. The speed of the WBC tended to increase with increasing angular velocity ($\omega$) and increasing injection rate ($S_O$). Therefore, SENJYU (1988) carefully checked the speed of the WBC in the test experiments and determined the ranges of $\omega$ and $S_O$ for the partial barrier experiments in the next section.

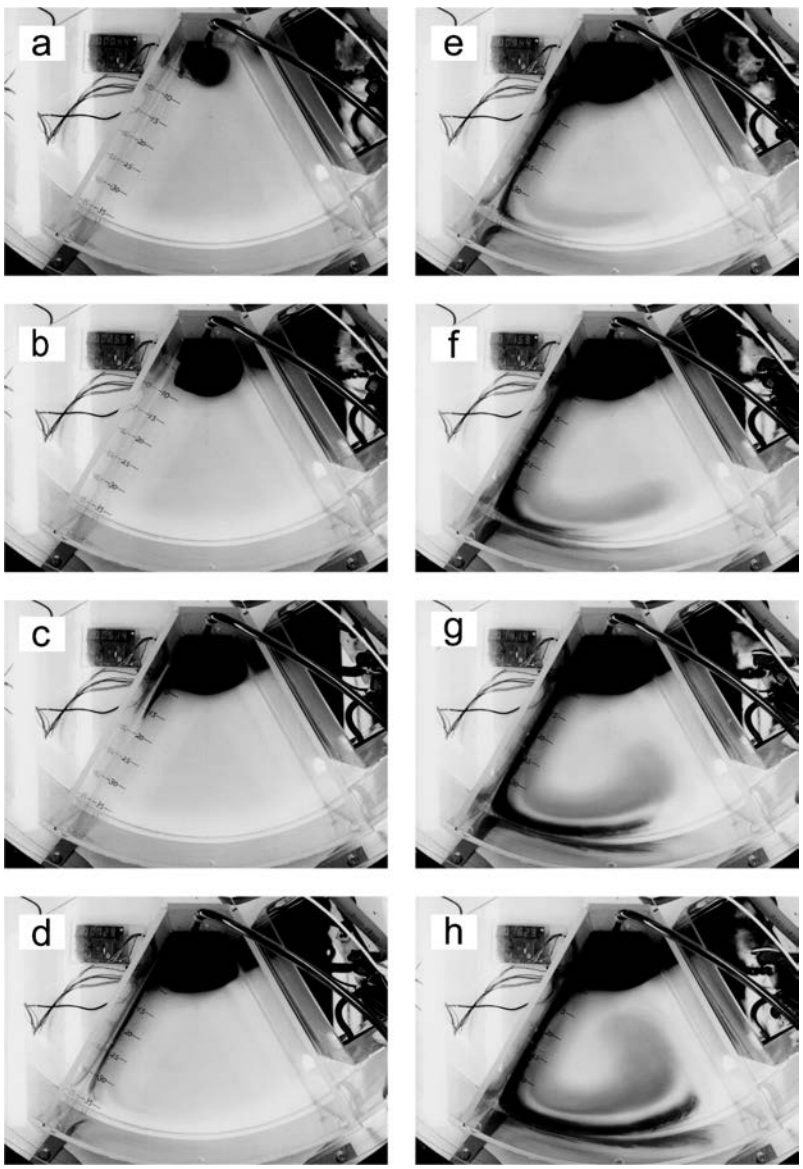


**Fig. 3** Results of a test experiment for the SA-type circulation ($S_O$= 1.5 $cm^3$ $s^{-1}$, $\omega$ = 0.79 rad $s^{-1}$). The photos show the distribution of dyed water at (a) 44 s (0.73 min), (b) 259 s (4.32 min), (c) 514 s (8.67 min), (d) 729 s (12.15 min), (e) 944 s (15.73 min), (f) 1159 s (19.32 min), (g) 1414 s (23.57 min), and (h) 1629 s (27.15 min) from the start of experiment.

## 3. Partial barrier experiments

For the partial barrier experiments, a meridional (radial) barrier extending from the rim (a flat acrylic board of 4 mm thickness) was attached in the tank in order to divide the sector into three basins: *N*, *SW*, and *SE* (Fig. 2). The

**Table 1.** Parameters for the partial barrier experiments

| | $S_O$ ($cm^3\ s^{-1}$) | $b$ (cm) | $B$ (= $b$/36 cm) | $\phi$ (°) | $\omega$ (rad $s^{-1}$) |
|---|---|---|---|---|---|
| Exp 1 | 0.2 | 15 | 0.42 | 30 | 0.79 |
| Exp 2 | 0.5 | 15 | 0.42 | 30 | 0.79 |
| Exp 3 | 1.0 | 15 | 0.42 | 30 | 0.79 |
| Exp 4 | 1.5 | 15 | 0.42 | 30 | 0.79 |
| Exp 5 | 1.0 | 10 | 0.28 | 30 | 0.79 |
| Exp 6 | 1.0 | 20 | 0.56 | 30 | 0.79 |
| Exp 7 | 1.0 | 15 | 0.42 | 20 | 0.79 |
| Exp 8 | 1.0 | 15 | 0.42 | 40 | 0.79 |
| Exp 9 | 1.0 | 15 | 0.42 | 30 | 0.70 |
| Exp 10 | 1.0 | 15 | 0.42 | 30 | 0.90 |

experimental parameters were length of the barrier ($b$) (we use a non-dimensional length scale $B$ which is the barrier length normalized by the radial extent of the tank, 36 cm) and angle of the barrier from the western boundary ($\phi$), as well as injection rate of water at the point source ($S_O$) and angular velocity ($\omega$) (Table 1). Basically, the changes of injection rate (Exps 1–4) and angular velocity (Exps 3 and 9–10) did not change the pattern of circulation. On the contrary, significant changes in flow pattern were observed depending on the length (Exps 3, 5–6) and the angle of the meridional barrier (Exps 3, and 7–8). Therefore, we show the results of Exps 3 and 5–8 below because our interest is how the SA-type circulation pattern in the previous section was modified by the partial barrier.

Firstly, the results of Exp 3 (the reference experiment) are shown in Fig. 4 using streak lines of the dyed injected water. In the first stage, the injected water formed a clockwise eddy of 12–15 cm diameter near the point source (1–3 min after the injection). Then, a narrow and fast flow along the western boundary appeared (4–5 min). We call this flow the WBC-N as this is the WBC in the *N*-basin. The WBC-N flowed into the *SW*-basin along the western boundary as the WBC-SW (6–7 min). The dyed water flowed eastward along the southern boundary accompanying northward flow component after arriving at the rim (8–16 min). The northward interior flow was wider but much slower than the WBC-SW. At this time, a westward intensified cyclonic gyre was confirmed in the *SW*-basin. Part of the northward flow turned to the east at the tip of the meridional barrier, then flowed into the *SE*-basin forming a WBC (the WBC-SE) (17–20 min). The water arrived at the rim in the *SE*-basin flowed along the southern boundary accompanying weak northward component, showing a cyclonic gyre similar to that in the *SW*-basin (21–27 min).

A clear cyclonic gyre was formed in both the *SW* and *SE*-basins even when the length of the barrier was changed (Figs. 4 and 5). However, in the case of Exp 5, the WBC-SE was significantly broad and the westward intensification in the *SE*-basin did not fully develop (Fig. 5a), though a similar westward intensified gyre was formed in the *SW* and *SE*-basins in Exps 3 and 6 (Figs. 4 and 5b). This suggests that the short barrier in Exp 5 did not work as a barrier. The circulation pattern possibly approaches the SA-type circulation in Fig. 3 with decreasing the length of the barrier. Contrary, water of the WBC-SE was directly supplied from the clockwise eddy at the point source in Exp 6 (Fig. 5b) as the tip of the barrier is near the source region.

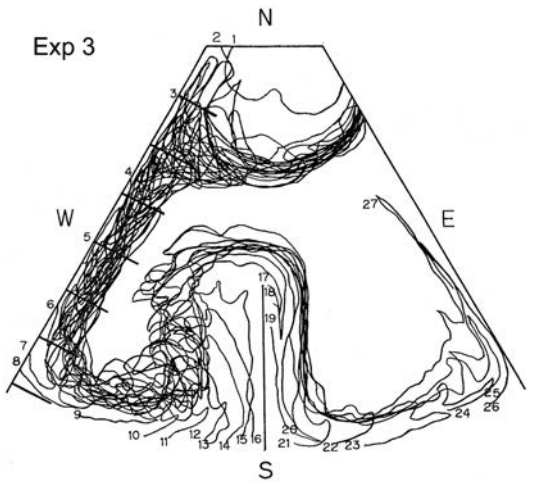


**Fig. 4** Flow pattern of Exp 3 (the reference experiment) visualized by the dyed water. The contours indicate streak of the injected dyed water every 1 min. Numerals show the elapsed time from the start of the experiment (min). The ruler on the western boundary is graduated at 5 cm.

In Exps 3 and 8, clear cyclonic gyre was formed in both the *SW* and *SE*-basins (Figs. 4 and 6b). In contrast, the gyre in the *SW*-basin was obscure in Exp 7, though a cyclonic gyre was found in the *SE*-basin (Fig. 6a). A reason for the obscure gyre in the *SW*-basin is that a zonal flow toward the *SE*-basin was separated from the WBC-N at 4–5 min and fed the WBC-SE together with the northward flow in the *SW*-basin. The volume of southward-flowing WBC equals the sum of the zonally-integrated northward interior flow and the volume of upwelling over the basin. Therefore, the volume of WBC-SE is larger than that of WBC-SW in Exp 7. In order to feed the larger volume of WBC-SE, the zonal flow was separated from the WBC-N. However, crossing of the zonal flow with the northward internal flows in the *SW*-basin disturbed the streak of dyed water, which resulted in the obscure gyre pattern in the basin.

## 4. Discussions

As pointed out earlier, the geometry of the partial barrier experiment is similar to the topography of the Japan Sea (Figs. 1 and 2). The *N*, *SW*, and *SE*-basins correspond to the Japan, Tsushima, and Yamato Basins, respectively. The meridional barrier coincides with the Yamato Rise and Oki Spur. In addition, the formation region of the Japan Sea Proper Water located on the northwestern Japan Basin (SENJYU and SUDO, 1993 & 1994; SENJYU *et al.*, 2002) agrees with the

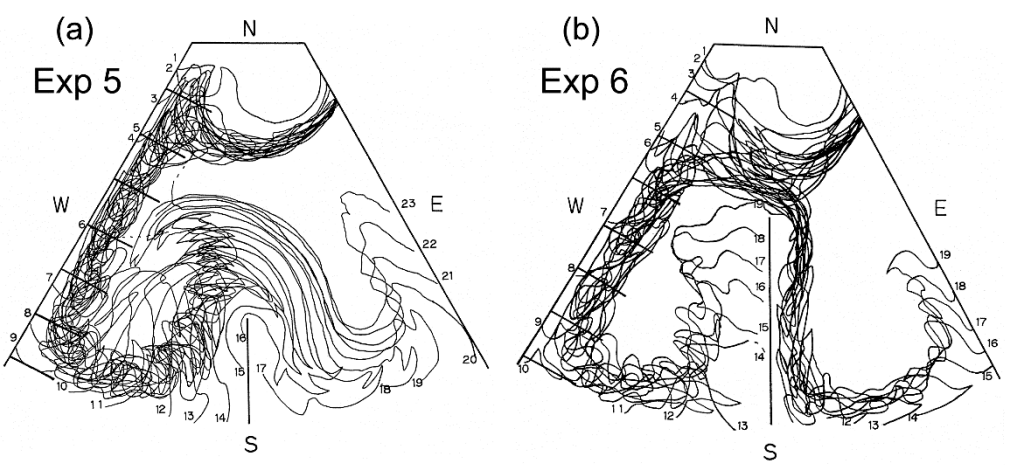


**Fig. 5** Same as Fig. 4 except for Exp 5 (a) and Exp 6 (b).

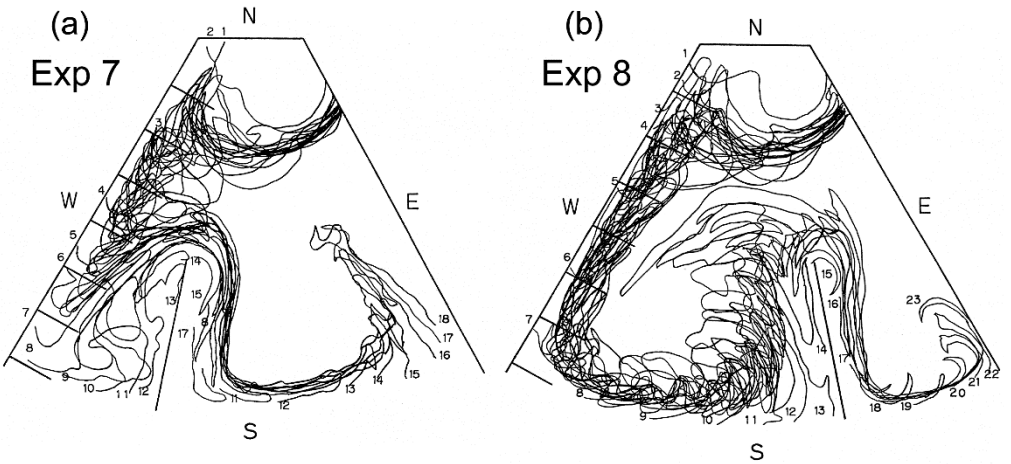


**Fig. 6** Same as Fig. 4 except for Exp 7 (a) and Exp 8 (b).

point source of the *N*-basin in the experiments. Therefore, if the bottom topography of the Japan Sea were flat, with the simple topography of the Yamato Rise and Oki Spur, similar circulation pattern to the experiments is expected in the abyssal Japan Sea.

Figure 7 shows the mean flow vectors in the abyssal Japan Sea (> 1000 m) from direct current observations; this is the updated version of Fig. 3b in SENJYU *et al.* (2005b) adding our new data as well as these of FUKUSHIMA and KOJIMA (2011) and TEAGUE et al. (2005). By comparing with the flow pattern of the partial barrier experiments (Figs. 4–6), we found several common features.

The first is the cyclonic circulation in the southern basins (the Tsushima and Yamato Basins). The cyclonic circulation has been interpreted as a flow trapped on the slope of the basin's periphery, seeing shallow region on its right-hand side (CHOI and YOON, 2010). In fact, the observed flows tend to follow the contours of ambient potential vorticity ($f$ / $H$, where $H$ is bottom depth), which indicates that the topographic $\beta$-effect is more important than the planetary $\beta$-effect.

The second common feature that is interesting is the strong currents along the western boundary in the southern basins. We can find strong flows faster than 3 cm $s^{-1}$ along the southeastern flank of the Yamato Rise in the Yamato Basin and the western periphery of the Tsushima Basin east of the Korean Peninsula. These strong flows are likely to be the WBC in each basin, a characteristic feature of the SA-type circulation.

The third common feature is that the water in the *SE*-basin is older than that in the *SW*-basin (FALLER, 1960). It has been considered that the Japan Sea Proper Water in the Yamato Basin is the oldest water in the Japan Sea, because it has the lowest concentration of dissolved oxygen in the sea (SUDO, 1986; GAMO *et al.*; 1986, SENJYU and SUDO, 1993 & 1994; SENJYU *et al.*, 2005a). However, the reason is probably different from the experiments. In the experiments, the WBC-SE was fed by the northward flow in the *SW*-basin, except in case of Exp 6 (Fig. 5b). While in the Yamato Basin, the deep and bottom waters are supplied directly from the Japan Basin, similar to Exp 6. It is meaningful that if we normalize the shallow ridge from the Yamato Rise to Oki Spur (about 560 km) by the latitudinal extent of the

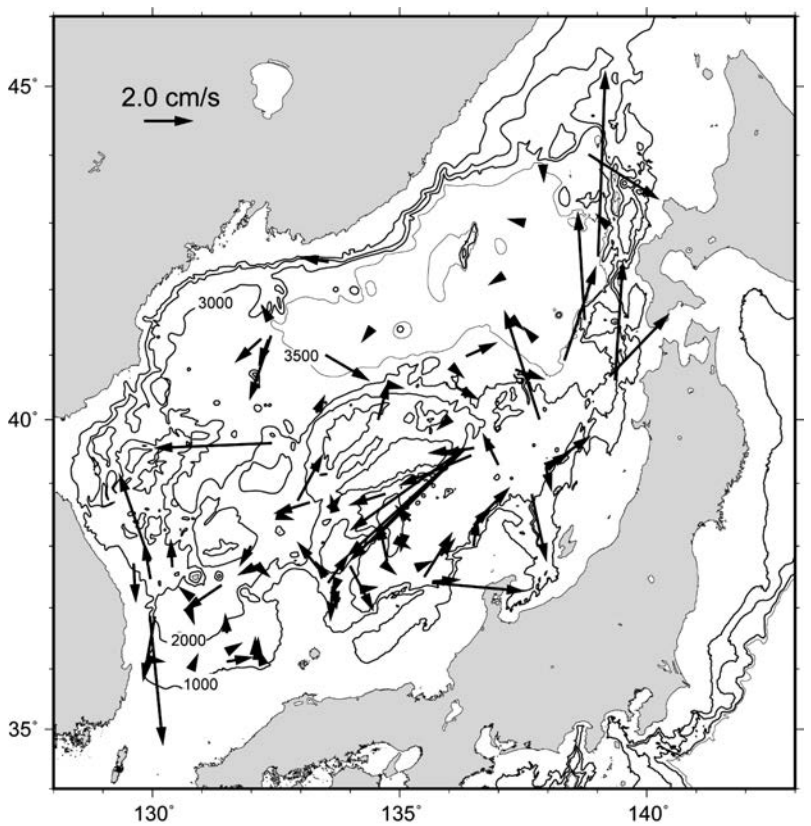


**Fig. 7** Distribution of the mean flow vectors in the abyssal Japan Sea (1000 m-bottom) from direct current observations. A vector length of 2.0 cm $s^{-1}$ is shown in the upper-left corner.

Japan Sea (roughly 1000 km), the non-dimensional length ($B$) is 0.56 as in Exp 6. Nevertheless, because of the narrow channel between the Japan and Yamato Basins, the water exchange between the basins is limited (SENJYU *et al.*, 2013, SENJYU *et al.,* 2017), and the water in the Yamato Basin is a modified water that has lower dissolved oxygen concentration due to the closed circulation in the basin (SENJYU *et al.*, 2005a, b).

However, there are many different points between the experiments and observations. For example, remarkable northward flows in the eastern Japan Basin cannot be explained by the SA-type circulation. The basic SA-type circulation is likely to be strongly modified not only by the complex bottom topography, but also by eddy activity (CHOI and YOON, 2010; YOSHIKAWA, 2012).

## 5 Concluding remarks

We have made a qualitative discussion throughout, focusing on the geometric similarity between the partial barrier experiments and the Japan Sea. There are several common features between the experiments and the observed deep flow field in the sea. The cyclonic circulation and strong currents near the western boundary in the Yamato and Tsushima Basins suggest the

SA-type circulation. However, the complex bottom topography and eddy activity are likely to modify the basic SA-type circulation pattern.

The key strategy to confirm the SA-type circulation in the Japan Sea is to perform observations of the deep WBC in the Japan Basin. However, it flows in the North Korean territory which is an inaccessible area due to political problems at present. Data analysis of neutral drifters, such as ARGO floats, may be an effective way. In addition, chemical tracer observations are useful in capturing the deep flow pattern. Hydrographic observations in a wide area including Russian and Korean territories are desired.

Nowadays, studying geophysical fluid dynamics with the help of rotating-tank experiments is somewhat out-of-date. However, in general, laboratory experiments have an advantage of providing an intuitive understanding of phenomena. Therefore, we believe that laboratory experiments including rotating-tank experiments are still valuable not only in the field of education but also in heuristic research, even though numerical model experiments have highly progressed.

**Acknowledgments**

This work is a contribution to the JY's retirement ceremony. TS wishes to thank Emeritus Professors Hideo Sudo and Masaji Matsuyama in Tokyo University of Fisheries (present Tokyo University of Marine Science and Technology) for useful discussion and encouragement in TS's master course student days. Part of this study was supported by the Environment Research and Technology Development Fund of Ministry of the Environment, Japan (2-1604) and JSPS KAKENHI Grant Number 18H03741.

**References**

BROECKER, W. S. and T.-H. PENG (1982): Tracers in the Sea. A publication of the Lamont-Doherty Geological Observatory, Colombia University, New York, 690 pp.

CHOI, Y. G. and J.-H. YOON (2010): Structure and seasonal variability of the deep mean circulation of the East Sea (Sea of Japan). J. Oceanogr., **66**, 349-361. doi:10.1007/s10872-010-0031-y.

FALLER, A. J. (1960): Further examples of stationary planetary flow patterns in bounded basins. Tellus, **12:2**, 159-171.

FUKUSHIMA, S. and T. KOJIMA (2011): Characteristics of deep current observed near the bottom in the Sea of Japan. Report of Hydrographic and Oceanographic Researches, Hydrographic and oceanographic department, Japan Coast Guard, **47**, 32-43.

GAMO, T. and Y. HORIBE (1983): Abyssal circulation in the Japan Sea. J. Oceanogr. Soc. Japan, **39**, 220-230.

GAMO, T., Y. NOZAKI, H. SAKAI, T. NAKAI and H. TSUBOTA (1986): Spatial and temporal variations of water characteristics in the Japan Sea bottom water. J. Mar, Res., **44**, 781-793.

KUO, H.-H. and G. VERONIS (1971): The source-sink flow in a rotating system and its oceanic analogy. J. Fluid Mech., **45** (3), 441-464.

LONG, R. R. (1954): Note on TAYLOR's "ink walls" in a rotating fluid. J. Meteor., **11**, 247-249.

SENJYU, T. (1988): Study on abyssal circulation by rotating-tank experiments. Master's thesis, Tokyo University of Fisheries, 71 pp. (unpublished manuscript)

SENJYU, T. and H. SUDO (1993): Water characteristics and circulation of the upper portion of the Japan Sea Proper Water. J. Mar. Sys., **4**, 349-362.

SENJYU, T. and H. SUDO (1994): The upper portion of the Japan Sea Proper Water; its source and circulation as deduced from isopycnal analysis. J. Oceanogr., **50**, 663-690.

SENJYU, T., T. ARAMAKI, S. OTOSAKA, O. TOGAWA M. DANCHENKOV, E. KARASEV and Y. VOLKOV (2002): Renewal of the bottom water after the winter 2000-2001 may spin-up the thermohaline circula-

tion in the Japan Sea. Geophys. Res. Lett., **29** (**7**), doi: 10.1029/2001GL014093.

SENJYU, T., Y. ISODA, T. ARAMAKI, S. OTOSAKA, S. FUJIO, D. YANAGIMOTO, T. SUZUKI, K. KUMA and K. MORI (2005a): Benthic front and the Yamato Basin Bottom Water in the Japan Sea. J. Oceanogr., **61**, 1047–1058, doi:10.1007/s10872-006-0021-2.

SENJYU, T., H. R. SHIN, J.-H. YOON, Z. NAGANO, H. S. AN, S. K. BYUN and C. K. LEE (2005b): Deep flow field in the Japan/East Sea as deduced from direct current measurements. Deep-Sea Res. II, **52**, 1726–1741. doi:10.1016/j.dsr2.2003.10.013.

SENJYU, T., T. ARAMAKI, S. S. TANAKA, J. ZHANG, Y. ISODA, Y. KUMAMOTO, S. HIBINO and T. NAKANO (2013): Abyssal water mass exchange between the Japan and Yamato Basins in the Japan Sea. J. Geophys. Res. Ocean, **118**, 4878–4888, doi: 10.1002/jgrc.20373.

SENJYU, T. and T. ARAMAKI (2017): Volume transport from the Japan Basin to the Yamato Basin in the abyssal Japan Sea inferred from direct current observations. J. Oceanogr., **73**, 235–247, doi: 10.1007/s10872-016-0399-4.

STOMMEL, H. (1958): The abyssal circulation. Deep-Sea Res., 5, 80–82.

STOMMEL, H., A. B. ARONS and A. J. FALLER (1958): Some examples of stationary planetary flow patterns in bounded basins. Tellus, **10:2**, 179–187.

STOMMEL, H. and A. B. ARONS (1960a): On the abyssal circulation of the world ocean- I. Stationary planetary flow patterns on a sphere. Dee-Sea Res., **6**, 140–154.

STOMMEL, H. and A. B. ARONS (1960b): On the abyssal circulation of the world ocean- II. An idealized model of the circulation pattern and amplitude in oceanic basins. Deep-Sea Res., **6**, 217–233.

SUDO, H. (1986): A note on the Japan Sea Proper Water. Prog. Oceanogr., **17**, 313–336.

SWALLOW, J. C. and L. V. WORTHINGTON (1961): An observation of a deep countercurrent in the western North Atlantic. Deep-Sea Res., **8** (**1**), 1–21.

TALLEY, L. D., G. L. PICKARD, W. J. EMERY and J. H. SWIFT (2011): Descriptive Physical Oceanography. An Introduction. Sixth Edition, Elsevier, MA, USA, ISBN: 978-0-7506-4552-2.

TEAGUE, W. J., K. L. TRACEY, D. R. WATTS, J. W. BOOK, K.-I. CHANG, P. J. HOGAN, D. A. MITCHELL, M.-S. SUK, M. WIMBUSH, J.-H. YOON (2005): Observed deep circulation in the Ulleung Basin. Deep-Sea Res. II, **52**, 1802–1826.

VERONIS, G. and C. C. YANG (1972): Nonlinear source-sink flow in a rotating pie-shaped basin. J. Fluid Mech., **51** (**3**), 513–527.

WELANDER, P. (1969): Effects of planetary topography on the deep-sea circulation. Deep-Sea Res., supp. **16**, 369–391.

YOSHIKAWA, Y. (2012): An eddy-driven abyssal circulation in a bowl-shaped basin due to deep water formation. J. Oceanogr., **68**, 971–983, doi:10.1007/s10872-012-0148-2.

*Received: August 1, 2018*
*Acccepted: December 21, 2018*